Short Lectures - E, Wednesday, June 13

SL - E1

MODELLING EFFECTS OF SMALL CRYSTALLITE SIZE AND LATTICE DEFECTS ON POWDER DIFFRACTION LINES

Z. Matěj, R. Kužel

Department of Condensed Matter Physics, Faculty of Mathematics and Physics, Charles University in Prague, Ke Karlovu 5, 121 16 Praha 2, Czech Republic
matej@karlov.mff.cuni.cz

Introduction

X-ray powder diffraction (XRPD) techniques are very appropriate for characterisation of various materials as non-destructive and containing rich information on phase composition, lattice parameters, crystal structure and other aspects of material structure on nanometre and submicrometer scale, which can be related to application properties and hence to be also of technological interest. Presence of lattice defects, their type and concentration as well as crystallite size can be determined from width and shape of diffraction lines. The aim of this contribution is to give a short overview of classical approaches of a line profile analysis (LPA) complemented with methods based on simulations and fitting of whole diffraction patterns advanced during the last decade. The theoretical summary is supplemented with some practical examples.

Direct and whole profile modelling techniques

Already at the birth of the XRD analysis *Scherrer* (1918) [1] utilized a simple relation between diffraction peak width and particle size. Variations of the lattice parameter between individual crystallites or lattice deformations around defects were then included in the *Williamson-Hall* plot method [1], which links information from multiple *hkl* reflections to separate the size and strain related broadening effects. Fourier transformation of intensity data and again the analysis of reflections of different order are the basis of the *Warren-Averbach* method [1]. This technique can reveal finer details in the real space without preliminary assumptions about the microstructure model.

Generally any LPA method introduces some approximations and indeed some of them require ill-posed steps, such us deconvolution. A common attribute of all the methods mentioned is that reflections in the powder pattern are analysed separately, which becomes problematic due to strong peak overlap especially in the case of nanocrystalline or low symmetry materials. It can be solved by introduction of the *Rietveld method*. All peaks in the diffraction pattern are fitted simultaneously on a basis of some model, which parameters are refined. Most of models used also by direct methods can be generalised and adapted also for the Rietveld technique. E.g. anisotropy (*hkl* dependence) of peak broadening can be accounted for any type of crystal symmetry [2,3]. For computational simplicity analytical profile function, e.g. pseudo-Voigt function, are utilized to describe peak profiles in the classical Rietveld programs. Nevertheless in many cases, see Fig. 1 showing peak broadening in fcc metal sample induced by stacking fault defects [4], peak shape can be quite complex. Hence it was proposed by Scardi&Leoni (2000) [5] and Ribárik& Ungár [6] to simulate shape of diffraction profiles from a microstructural model suitable for a particular material and problem under investigation. This technique of the *whole powder pattern modelling* (WPPM) makes it possible to determine e.g. stacking fault probabilities or dislocation densities in severely deformed (SPD) metals [6].

At first the WPPM method was applied to some model cubic [5-6] or hexagonal materials. However, as in the last decade mainly nano-materials stay in the centre of interest, validity of an additional approximation present also in WPPM was discussed. This important assumption is known in Warren [1] as a "powder diffraction theorem" or in Beyerlein (2011) [7] as a "tangent plane approximation". The problem can be intrinsically solved if the powder pattern is calculated from the atomistic model using a well known *Debye formula*. This technique can be used for calculation of scattering from various nano-objects as nanotubues [8] etc., but it is hardly scalable to larger 3D objects because of its computational complexity.

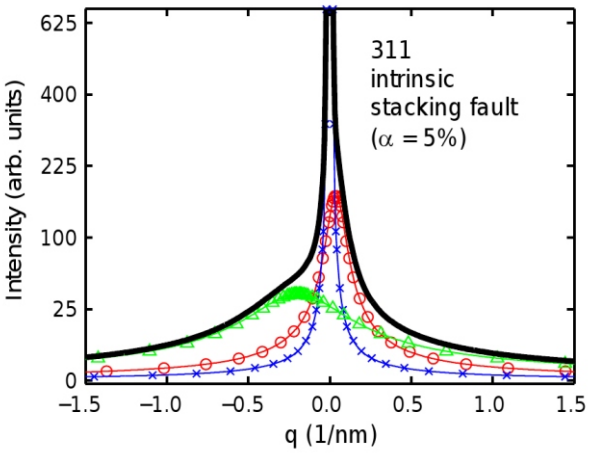

Figure 1. Simulated diffraction profile for a fcc copper polycrystalline specimen with intrinsic stacking faults. 311 reflection, stacking fault probability = 0.05. Thick black line depicts the whole diffraction profile. Colour lines show its subcomponents. The stacking fault effect was convoluted with size broadening to avoid the delta peak from unaffected components. Crystallites size was set to D 200 nm. Similar figure can be seen in Balogh et al. [4]. ($q = 4 \sin / $).

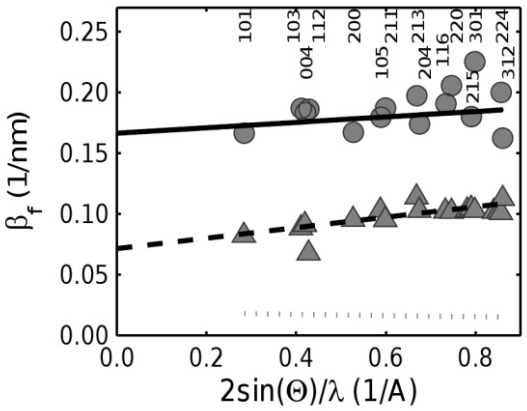

Figure 2. Williamson-Hall plot of a TiO_2 sample prepared by hydrolysis of *n*-butoxide [11] at temperature 300 °C (circles) and at 450 °C (triangles).The integral breadths of anatase reflection with instrumental broadening already deconvoluted are plotted. It has to be also considered that there is a very strong peak overlap - especially for the sample prepared at 300 °C (see Fig. 4).

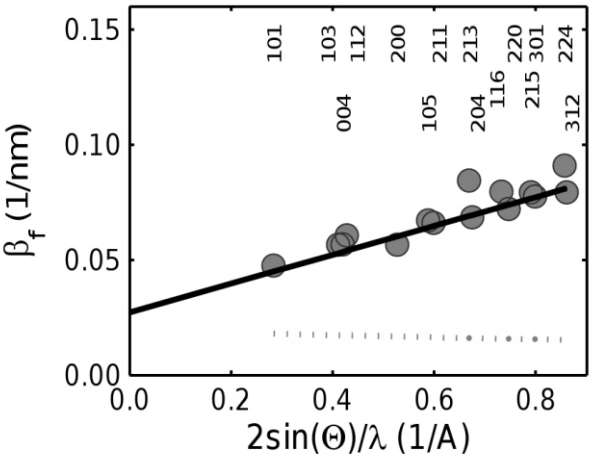

Figure 3. Williamson-Hall plot of a TiO_2 sample prepared by hydrolysis of isopropoxide [11] at temperature 400 °C. A significant microstrain broadening is evident.

Lattice defects

In WPPM the microstructural models are usually build in the real space, where Fourier coefficients are derived and the profile is calculated by means of Fourier transformation. In this contribution a formalism introduced by Wilkens [9] and Krivoglaz & Ryaboshapka [10] for *dislocation induced broadening* will be briefly presented. Its application will be demonstrated on *SPD copper samples* and *nanocrystalline metal samples*, where also stacking fault defects (Fig. 1) play an important role.

Nanostructures and size effects

Determination of *crystallite size distribution* will be illustrated on *model TiO_2 samples* prepared by different chemical routes. Nevertheless in these samples the broadening effect is dominating (Fig. 2), it should be borne in mind that

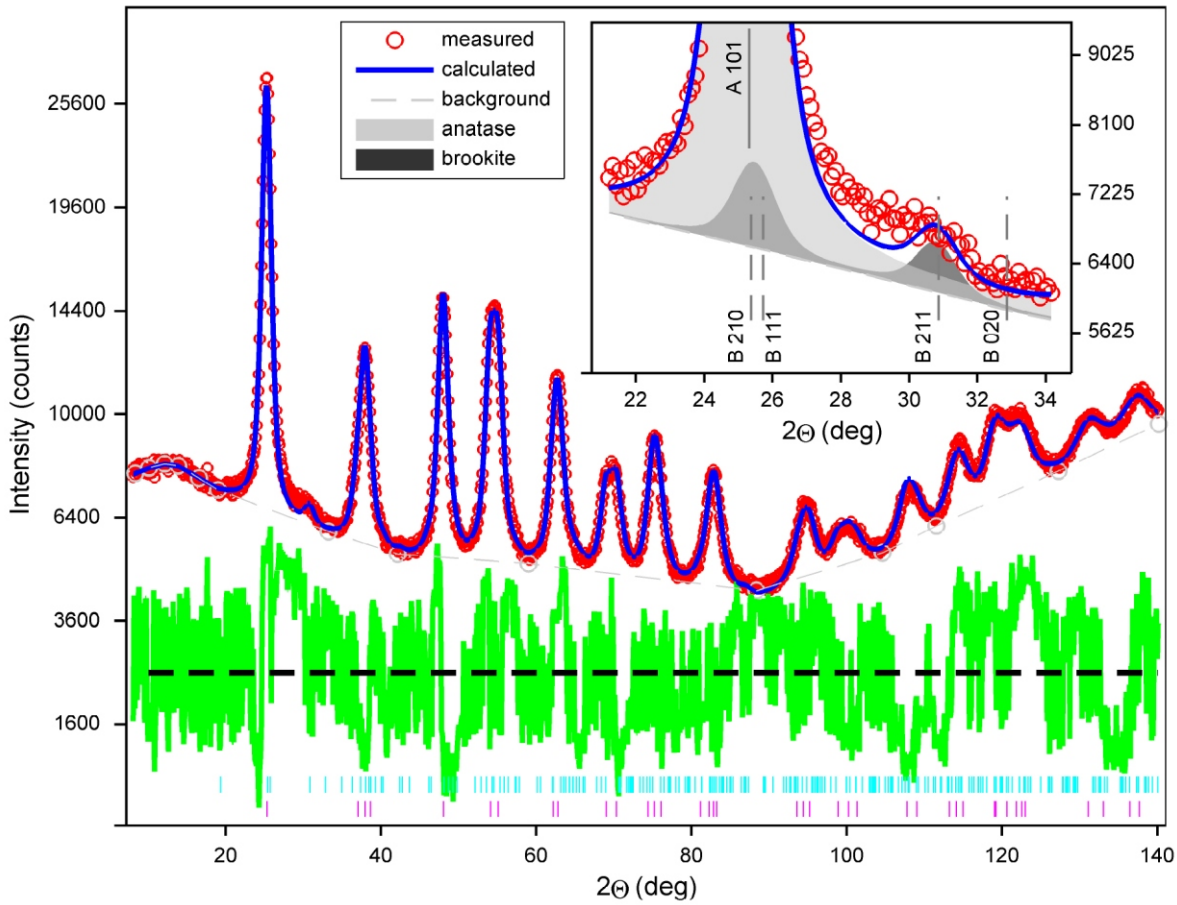

Figure 4. Pattern fit of a TiO_2 sample prepared by hydrolysis of *n*-butoxide at temperature 300 °C [11]. Small magenta ticks at the bottom mark the anatase reflections, whereas the cyan ticks above indicate reflections from the minor phase (here brookite).

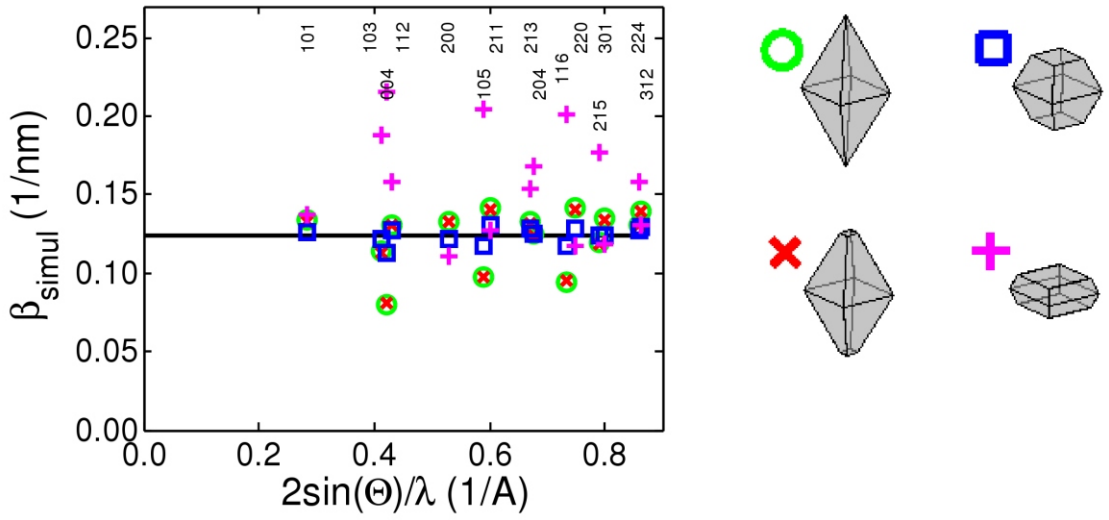

Figure 5. Simulated Williamson-Hall plots for anatase crystallites of bipyramidal shape and different areas ratio of {101} and {001} facets. It is visible that some particular configurations (depicted by squares) are hardly distinguishable from the isotropic one for the spherical crystallites (line).

also presence of microstrain can not be always neglected (Fig. 3). A pattern fit of a model samples is depicted in Fig. 4. Beside the approximations mentioned above also an effect of *crystallite shape* will be discussed (Fig. 5).

Other effects

When compared to the direct methods analysing reflections separately, the whole powder pattern modelling techniques have also a significant drawback. There is complex information encoded by nature in the experimental pattern. The direct methods can simply separate individual effects, by neglecting their mutual influence in the analysis, e.g. it is assumed that reflection position is not related to its width and shape. Contrary the whole pattern fitting procedure has to account for several effects mixed together to reach good pattern fit and reliable results. Background scattering, *residual stresses* and *texture* have to be also included.

Computer programs

There are many *computer programs* suitable for modelling powder diffraction profiles. Some of them (PM2k [12], Maud [13] and MStruct [14]) will be briefly introduced.

References

1. B. E. Warren, *X-ray Diffraction.* Addison-Wesley. 1969.
2. N. C. Popa, *J. Appl. Cryst.*, **31**, (1998), 176.
3. P. W. Stephens, *J. Appl. Cryst.*, **32**, (1999), 281.
4. L. Balogh, G. Ribárik, T. Ungár, *J. Appl. Phys.*, **100**, (2006), 023512.
5. P. Scardi, M. Leoni, *Acta Cryst. A*, **58**, (2002), 190.
6. G. Ribárik, T. Ungár, J. Gubicza, *J. Appl. Cryst.*, **34**, (2001), 669.
7. K. R. Beyerlein, R. L. Snyder, P. Scardi, *J. Appl. Cryst.*, **44**, (2011), 945.
8. T. Brunátová, S. Daniš, R. Kužel, D. Králová, *Z. Kristallogr. Proc.*, **1**, (2011), 229.
9. M. Wilkens, in *Fundamental aspects of dislocation theory*, **317**, (1970), 1191.
10. M. A. Krivoglaz, *X-Ray and Neutron Diffraction in Nonideal Crystals.* Springer. 1996.
11. L. Matějová, Z. Matěj, O. Šolcová, *Micro. Mesoporo. Materials*, **154**, (2012), 187.
12. M. Leoni, T. Confente, P. Scardi, *Z. Kristallogr. Suppl.*, **23**, (2006), 249.
13. L. Lutterotti, M. Bortolotti, *IUCr: Comput. Commission Newsletter*, 1, (2003), 43, www.ing.unitn.it/~maud.
14. Z. Matěj, *Materials Struct. Chem. Biol. Phys. Tech.*, 17-2a, (2010), k99, xray.cz/mstruct.

SL -E2

THE PROGRAM FOR MACROSCOPIC STRESS ANALYSIS

J. Drahokoupil

Faculty of Nuclear Science and Physical Engineering in Prague; Trojanova 13, 120 00 Prague 2, Czech Republic
jan.drahokoupil@fjfi.cvut.cz

The program, written in Microsoft Excel, is based on "General least-square analysis" [1]. The general equation (1) for macroscopic stress is used. Thus, no limitations for angles are used as is for example in method $\sin^2$ plot or its modification [2].

$$^{hkl} \quad 1/\,2S_2^{hkl}[(\ _{11}\cos^2 \quad _{12}\cos^2 \quad \sin^2 \quad _{33}\cos^2$$
$$(\ _{13}\cos^2 \quad _{23}\cos^2 \quad \sin 2\ ]\ \ S_1^{hkl}(\ _{11} \quad _{22} \quad _{33})$$

The program features can be summarized as:

- Data from different diffractometers with various wavelengths can be used together in one computation of stress tensor. The correction for sample displacement and zero shift errors are also included.
- The program is very appropriate for description of strain depth gradients. All stress tensor component are described by polynomial representation (to fourth order) as function of depth.
- The program also enable to determinate the lattice parameter also with it depth evolution. The polynomial representation (to second order) for lattice parameter is used. See section deep averaging in chapter 3.10.
- The elastic anisotropy is described by Neerfeld-Hill model with weight factor between Reuss and Voight models. The weight factor can be also determined from refinement. For cubic symmetry is enough to enter only the elastic constants c_{11}, c_{12} and c_{14} and the X-ray elastic constants are computed on the base of *hkl*. For non-cubic symmetry for every used *hkl* the X-ray elastic constants has to be entered.
- If experimental data was collected at various temperatures the program enables correction for it using linear coefficient of temperature expansion.
- The data collected from different depth can be used for the stress tensor determination with depth gradients.
- Two kind of graphical output are pre-constructed. The $\sin^2$ plot is used for visual comparison between measured and computed experimental data. For review of correctness all components of stress tensor are plotted as function of depth.
- The program is connecting strain, stress and temperature effect on inter-planar distance and as such is not only limited to macroscopic stress analysis but it can work in opposite way or the material constant can be variables (e.g.: from known stresses and strains the elastic constants can be determined; from known temperatures and inter-planar distances the linear coefficient of thermal expansion can be determined).

The program is relatively complex and is not suitable for beginners in macroscopic stress analysis since the number of refinable parameters is larger than information given by position of usually measured peaks. Nevertheless, for experienced user can offer very appropriate tool for his research. Moreover, the big advantage of the program is that it can be easily modified by user with standard knowledge of Microsoft Excel program.

This research was supported by the project FR-TI3/814 of Ministry of Industry and Trade of the Czech Republic.

1. R.A. Winholtz, J.B. Cohen, *Aust. J. Phys.*, **41**, (1988), pp. 189-199.
2. V. Hauk, Editor., Structural and Residual Stress Analysis by Nondestructive Methods. Amsterdam: Elsevier, (1997).

SL - E3

APPLICATION OF DIFFRACTION PATTERN REFINEMENT SOFTWARE FOR ANALYSES OF OXIDE LAYERS ON REFRACTORIES

M. Černík, S. Štulrajter, J. Bounziová

U. S. Steel Košice, s.r.o., Útvar GM pre výskum a vývoj USSE, 044 54 Košice, Slovak Republic
mcernik@ sk.uss.com, sstulrajter@ sk.uss.com, jbounziova@ sk.uss.com

Refractories used in the push furnace and casting ladles are not only exposed to high temperatures, but also to the oxide materials, which are present in liquid slag and steel. Knowledge about changes in the structure in that part of the refractories, which come into contact with the liquid slag, has practical importance in operation of these facilities. The numerous refractories are used in real practice, which have a common basis consisting of single oxides such as Al_2O_3, MgO, CaO, ZrO_2, SiO_2 etc., because these materials together with the carbon melt at high temperatures.

Oxides forming the slag based on elements as: Fe, Al, Ca, Si, Mg, Na, K etc., in many cases significantly affect on the basic refractory materials. A number of new minerals and phases with real structures form in the affected interactive locations, their heterogeneity and ability to penetrate into the structure of basic refractories is the subject of continuous study, in which X-ray diffraction method is very useful. The refinement of X-ray records by Rietveld method is considered an essential practice of real material structure study. The TOPAS and AutoQuant software, which were employed to clarify the diffraction patterns are very powerful tools and allow solving a very difficult tasks. In normal use of the Search-Match programs, it have been considered as good results when 3 to 5 phase were qualitatively determined from the diffraction record, currently the software combination allows accurate and quantitative determination of more then 10 phases in diffraction records. Experience shows that it is possible and necessary. In the figure 1 is shown an example the diffraction pattern of the refractory material in affected area, which in pure form contained only 75% Al_2O_3, 18% SiO_2 and 5% ZrO_2.

The reality of structure has been shown also with change of lattice parameter, which depends on material type and on the distance from the oxide layer surface. These changes can be observed mainly in the spinel structure. Changes in spinel structure affected by oxide layer are qualitatively and quantitatively presented for selected refractories.

1. J. Staroň, F. Tomšu, *Žiaruvzdorné Materiály Výroba, Vlastnosti a Použitie.* Slovmag a SMZ. 2000.

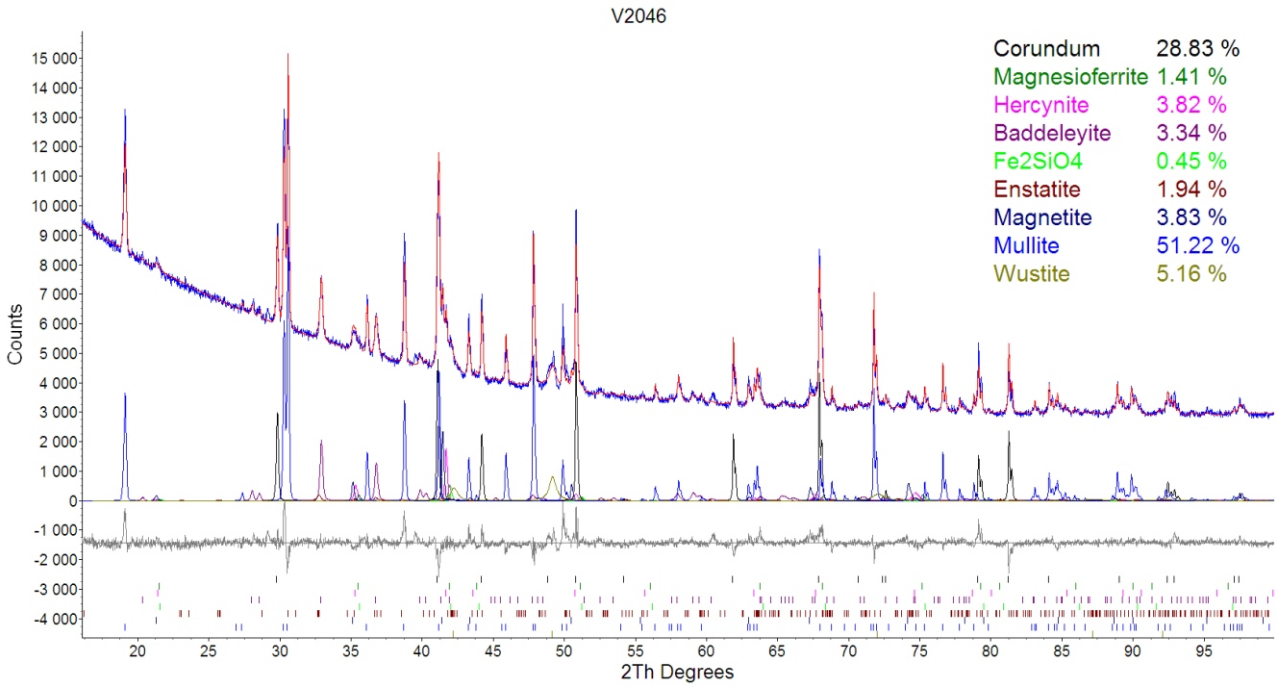

Figure 1. X ray record from the affected area of refractory material.